



Published in final edited form as:

Toxicol Sci. 2005 December ; 88(2): 630–644.

Role of Organic Anion and Amino Acid Carriers in Transport of Inorganic Mercury in Rat Renal Basolateral Membrane Vesicles: Influence of Compensatory Renal Growth

Lawrence H. Lash^{*},¹, Sarah E. Hueni^{*}, David A. Putt^{*}, and Rudolfs K. Zalups[†]

^{*} Department of Pharmacology, Wayne State University School of Medicine, Detroit, Michigan 48201;

[†] Division of Basic Medical Sciences, Mercer University School of Medicine, Macon, Georgia 31207

Abstract

Susceptibility to renal injury induced by inorganic mercury (Hg^{2+}) increases significantly as a result of compensatory renal growth (following reductions of renal mass). We hypothesize that this phenomenon is related in part to increased basolateral uptake of Hg^{2+} by proximal tubular cells. To determine the mechanistic roles of various transporters, we studied uptake of Hg^{2+} , in the form of biologically relevant Hg^{2+} -thiol conjugates, using baso-lateral membrane (BLM) vesicles isolated from the kidney(s) of control and uninephrectomized (NPX) rats. Binding of Hg^{2+} to membranes, accounted for 52–86% of total Hg^{2+} associated with membrane vesicles exposed to HgCl_2 , decreased with increasing concentrations of HgCl_2 , and decreased slightly in the presence of sodium ions. Conjugation of Hg^{2+} with thiols (glutathione, L-cysteine (Cys), N-acetyl-L-cysteine) reduced binding by more than 50%. Under all conditions, BLM vesicles from NPX rats exhibited a markedly lower proportion of binding. Of the Hg^{2+} -thiol conjugates studied, transport of $\text{Hg}-(\text{Cys})_2$ was fastest. Selective inhibition of BLM carriers implicated the involvement of organic anion transporter(s) (Oat1 and/or Oat3; *Slc22a6* and *Slc22a8*), amino acid transporter system ASC (*Slc7a10*), the dibasic amino acid transporter (*Slc3a1*), and the sodium-dicarboxylate carrier (SDCT2 or NADC3; *Slc13a3*). Uptake of each mercuric conjugate, when factored by membrane protein content, was higher in BLM vesicles from uninephrectomized (NPX) rats, with specific increases in transport by the carriers noted above. These results support the hypothesis that compensatory renal growth is associated with increased uptake of Hg^{2+} in proximal tubular cells and we have identified specific transporters involved in the process.

Keywords

Mercury-thiol conjugates; kidney; basolateral membrane vesicles; transport; organic anion transporters; amino acid transporters; compensatory renal growth

INTRODUCTION

Inorganic mercury (Hg^{2+}) is a potent and selective nephrotoxicant that accumulates primarily in the proximal tubular segments of the nephron (Barfuss *et al.*, 1990; Tanaka-Kagawa *et al.*, 1993; Zalups, 1991a, 1991b; Zalups and Barfuss, 1990). Uptake of Hg^{2+} by proximal tubular epithelial cells is mediated by transport proteins present in both luminal and basolateral plasma membranes (Zalups, 2000). Based on the distribution of plasma thiols and the high bonding-

¹ To whom correspondence should be addressed at Department of Pharmacology, Wayne State University School of Medicine, 540 East Canfield Avenue, Detroit, MI 48201. Fax: (313)-577-6739. E-mail: l.h.lash@wayne.edu..

affinity between mercuric ions and the reduced sulfhydryl group or thiolate anion, mercuric conjugates of albumin, L-cysteine (Cys), and glutathione (GSH) are likely biologically relevant forms of Hg^{2+} present in the renal circulation. Mercuric conjugates of N-acetyl-L-cysteine (NACys) may also be present in blood due to hepatic metabolism and may prove to be important molecular species taken up at the basolateral membrane (BLM) of proximal tubular epithelial cells (Zalups, 1998a; Zalups and Barfuss, 1998a). Overall, though, the di-cysteine S-conjugate of mercury, (R)-2-amino-3-((R)-2-amino-2-carboxy-ethylsulfanylmercurisulfanyl) propionic acid ($\text{Hg}(\text{Cys})_2$), is likely one of the primary forms of Hg^{2+} transported by renal proximal tubular epithelial cells (Lash *et al.*, 1998; Zalups and Barfuss, 1995a, 1998a; Zalups and Lash, 1997; Zalups and Minor, 1995).

Many carrier proteins in the plasma membrane have broad and often overlapping substrate specificities. Although certain molecules may be considered primary physiological substrates for a specific transporter, other molecules that are structural analogs of these substrates may also be transported by the same carrier protein. Zalups and colleagues (Cannon *et al.*, 2000; Zalups, 2000) proposed that $\text{Hg}(\text{Cys})_2$ and cystine serve as molecular homologs or mimics of one another at the sites of amino acid transporters involved in the absorptive transport of cystine.

Various methods have been used recently to identify plasma membrane carrier proteins that mediate transport of mercuric conjugates of biologically relevant thiols into renal proximal tubular cells (Aslamkhan *et al.*, 2003; Zalups, 2000). For example, competitive inhibition of the basolateral uptake of $\text{Hg}(\text{Cys})_2$ by *p*-aminohippurate (PAH) has implicated organic anion transporters (OAT1 and/or OAT3; *Slc22a6* and *Slc22a8*, respectively) in the basolateral uptake of mercuric species along the proximal tubule (Zalups, 1995, 1998b; Zalups and Barfuss, 1995b; Zalups and Minor, 1995). Organic ion transporter proteins also appear to participate in the transport of the GSH S-conjugate of trichloroethylene (Lash and Jones, 1985a), suggesting that mercuric conjugates of GSH may also be transportable substrates of these carrier proteins (Lash *et al.*, 1998; Zalups and Barfuss, 1995c).

More direct evidence for a role of OAT1 in the transport of $\text{Hg}(\text{Cys})_2$, the di-glutathione S-conjugate of inorganic mercury, (S)-2-amino-4-[(R)-2-[(R)-2-((S)-4-amino-4-carboxybutyrylamino)-2-(carboxymethyl-carbamoyl)-ethylsulfanylmercurisulfanyl]-1-(carboxymethyl-carbamoyl)-ethylcarbamoyl] butyric acid ($\text{Hg}(\text{GSH})_2$), and the di-N-acetyl-L-cysteine S-conjugate of inorganic mercury, (R)-2-acetylamino-3-((R)-2-acetylamino-2-carboxy-ethylsulfanylmercurisulfanyl) propionic acid ($\text{Hg}(\text{NACys})_2$), comes from recent studies in which MDCK cells were transfected stably with human OAT1 (Aslamkhan *et al.*, 2003; Zalups and Ahmad, 2004; Zalups *et al.*, 2004). As compared to control MDCK cells, the transfected cells more readily transported these mercuric species and became more readily intoxicated by the mercuric conjugates. A role for the BLM sodium-dicarboxylate transporter (SDCT2 or NADC3; *Slc13a3*) has also been implicated in the transport of Hg^{2+} -thiol conjugates in competitive inhibition experiments using small dicarboxylic acids (Zalups and Barfuss, 1998b, 2002).

A significant reduction in functional renal mass combined with compensatory renal cellular hypertrophy increases the susceptibility of the remaining functional renal mass to the nephropathy induced by exposure to Hg^{2+} (Houser and Berndt, 1986; Zalups, 1997; Zalups and Diamond, 1987; Zalups and Lash, 1990). Proximal tubular epithelial cells isolated from uninephrectomized (NPX) rats are also more sensitive to cellular injury induced by Hg^{2+} than those isolated from normal rats (Lash and Zalups, 1992; Lash *et al.*, 1999). This enhanced sensitivity appears to be associated with enhanced uptake and accumulation of Hg^{2+} (Houser and Berndt, 1988; Zalups, 1991a; Zalups and Lash, 1990; Zalups *et al.*, 1987), suggesting that

membrane proteins involved in the transport of mercuric species play a regulatory role in the expression of the toxic effects of Hg^{2+} .

We hypothesize that the mechanism by which compensatory renal growth causes increased accumulation of Hg^{2+} in proximal tubular epithelial cells is by increased activities of specific transporters of mercuric species at the luminal and/or basolateral plasma membrane. In the present study, we used the model of BLM vesicles isolated from kidney(s) of control and NPX rats to test the hypothesis that rates of basolateral transport of biologically relevant forms of Hg^{2+} increase significantly as a result of compensatory renal growth. Isolated membrane vesicles from kidney(s) of control and NPX rats are presently the most appropriate model to address this hypothesis. Other models, such as cell lines expressing specific carrier proteins, cannot reveal innate differences that result from the compensatory hypertrophy process that occur at the cellular and/or membrane level. Additionally, other methodological approaches, such as analysis of carrier expression by Western blotting, are problematic because only antibodies for some of the potential carriers are available and this will not provide information about post-translational modifications of carriers that may occur after compensatory renal growth. The present findings provide direct mechanistic support for the overall hypothesis, and identify specific carriers that are involved in the BLM transport of $\text{Hg}-(\text{Cys})_2$, $\text{Hg}-(\text{GSH})_2$, and $\text{Hg}-(\text{NACys})_2$.

METHODS

Experimental design—The overall goal of the present study was to test the hypothesis that “compensatory renal growth causes an increase in the activity of BLM carrier proteins that transport Hg^{2+} into proximal tubular epithelial cells.” Hg^{2+} is ostensibly never presented to the kidneys as a free, unbound mercuric ion, but rather, is bound in a coordinate covalent manner to one or more types of molecules possessing a reduced sulfhydryl group (Zalups and Lash, 1994). Evidence from several studies indicates that $\text{Hg}-(\text{Cys})_2$ is likely one of the primary physiological forms of Hg^{2+} transported into proximal tubular epithelial cells. Furthermore, evidence indicates that mercuric conjugates of GSH and NACys are also physiologically relevant forms of Hg^{2+} that may be transported across the BLM.

To insure that all of the mercuric ions in solution were bonded in a linear II coordinate manner to the sulfur atom of the desired thiol being studied, HgCl_2 was mixed in a 1:3 molar ratio with Cys, GSH, or NACys. Although Hg^{2+} -thiol conjugates formed in solution are forms of Hg^{2+} putatively transported into renal proximal tubular cells, we measured both the binding and transport of Hg^{2+} when it was in the form of HgCl_2 to provide a baseline for comparisons of binding and transport with Hg^{2+} -thiol conjugates and for comparison with previous findings from our laboratories (Zalups and Lash, 1997).

In addition to investigating the binding and transport of HgCl_2 and Hg^{2+} -thiol conjugates in isolated BLM vesicles from control and NPX rats, the present study delved further into the mechanisms involved in the basolateral transport of Hg^{2+} in proximal tubular epithelial cells by dissecting and separating the roles of five renal BLM transport systems in mediating the changes in Hg^{2+} -thiol transport associated with compensatory renal growth secondary to a significant reduction in renal mass. Transport and binding were measured in both the presence and absence of Na^+ ions, replacing NaCl with choline chloride for Na^+ -free incubations. Potential roles of specific carriers were assessed by incubating BLM vesicles simultaneously with 20 μM of a Hg^{2+} -thiol conjugate and 500 μM of a characteristic substrate for each carrier. In some of the incubation conditions, combinations of characteristic carrier substrates, each at 500 μM , were used to further assess the simultaneous function of multiple carriers. The five carriers (or carrier families) studied, with their Na^+ dependence and selective substrate indicated in parentheses, were: (1) The organic anion transporters (OAT1 [*Slc22a6*] and/or

OAT3 [*Slc22a8*]; indirect Na⁺ dependence; PAH and glutarate); (2) the sodium-dicarboxylate 2 (SDCT2 or NaDC3) carrier (*Slc13a3*; Na⁺-dependent; glutarate); (3) the amino acid transporter, system ASC (*Slc7a10*; Na⁺-dependent; L-alanine); (4) the dibasic amino acid transporter (DBAT, *Slc3a1*; Na⁺-dependent; L-lysine); and (5) the amino acid transporter, system L (*Slc7a1/2*; Na⁺-independent; L-phenylalanine). To promote the activity of OAT1 and OAT3, all BLM vesicles were prepared in the presence of 500 μM α-ketoglutarate, which is the principal intracellular substrate that drives the activity of OAT1 and OAT3 *in vivo*. This was accomplished by adding the α-ketoglutarate in the buffer at the step when pooled fractions identified as the BLM-fractions were centrifuged to remove Percoll and to concentrate the membrane vesicles (see below).

Studies using HgCl₂ or Hg-(GSH)₂ were performed with both untreated BLM vesicles and BLM vesicles pretreated for 15 min with 0.25 mM L-(αS,5S)-α-amino-3-chloro-4,5-dihydro-5-isoxazoleacetic acid (acivicin; both in the absence and presence of Na⁺ ions) to evaluate the role of γ-glutamyltransferase (GGT) in the transport process.

Materials—Percoll, PAH, acivicin, and L-γ-glutamyl-L-glutamate were purchased from Sigma Chemical Co. (St. Louis, MO). ²⁰³HgCl₂ (specific activity 8–12 mCi/mg Hg²⁺) was produced by previously described methods (Aslamkhan *et al.*, 2003). Radioactivity of ²⁰³Hg²⁺ was determined by gamma spectroscopy at a counting efficiency of ~50%. All other chemicals were of the highest purity available and were purchased from commercial sources.

Animals—Male Sprague-Dawley rats (175–200 g at time of surgery; Harlan Sprague-Dawley, Indianapolis, IN) were used in the present study. Animals were housed in the Wayne State University vivarium, were allowed access to laboratory chow and water *ad libitum*, and were kept in a room on a 12-h light-dark cycle. The rats were divided into two surgical groups; one that underwent uninephrectomy (NPX rats) and the other that served as a nonsurgical control. Animals undergoing uninephrectomy were anesthetized with a single ip injection of sodium pentobarbital (50 mg/kg body weight) before surgery. A right-sided uninephrectomy was performed as described previously (Zalups and Lash, 1990). Earlier studies (Zalups, 1991a, 1991b; Zalups and Diamond, 1987) showed that there are no ostensible differences in structural and functional parameters between the kidneys of untreated control rats and sham-operated rats. Hence, nonsurgically treated rats were used as controls. Animals were allowed to acclimate for at least 5 days before being used in the study. Rats that had undergone uninephrectomy (NPX rats) were not used until at least 10 days post-surgery to allow for completion of the rapid phase of compensatory renal growth.

Isolation of renal BLM vesicles—Rats (either control or NPX) were anesthetized with sodium pentobarbital (50 mg/kg body weight, ip). After achievement of anesthesia, the kidney (s) was (were) excised through a midline incision and placed quickly in ice-cold, Na⁺-free 10 mM triethanolamine/HCl buffer (pH 7.6) containing 250 mM sucrose and 0.1 mM phenylmethylsulfonyl fluoride (to inhibit proteolysis). Renal tissue, consisting of the cortex and outer stripe of the outer medulla, was obtained by careful dissection. The same buffer was used throughout, with additions as indicated.

Basolateral membrane vesicles were prepared by a modification of the Percoll density-gradient centrifugation procedure of Scalera *et al.* 1981. Renal tissue (approximately 2 to 3 g) was homogenized in a Dounce homogenizer, containing 30 ml of buffer, with a serrated Teflon pestle (1200 rpm, 30 strokes, clearance of 0.15 to 0.23 mm; Arthur Thomas Co., Philadelphia, PA). An additional 20 ml of buffer were added to the homogenate, and then the total volume of homogenate was divided equally into two 50-ml polycarbonate, round-bottom centrifuge tubes. All steps were performed at 4°C. The homogenate was centrifuged at 2500 × g for 15 min. Supernatants were decanted into two new centrifuge tubes and centrifuged at 20,000 ×

g for 30 min to obtain the fluffy layer, which consists of crude plasma membranes. The fluffy layer was resuspended in 30 ml of buffer and then was homogenized gently in a Dounce homogenizer. Percoll (3 ml; final concentration = 10%, v/v) was then added to 27 ml of the homogenate containing crude plasma membranes. This mixture was homogenized gently and then centrifuged in 50-ml polycarbonate, round-bottom centrifuge tubes at $48,000 \times g$ for 30 min. The gradient was fractionated from the top by pumping a 60% (w/v) sucrose solution (which was colored with blue dextran [3 mg/50 ml]) to the bottom of the tube through an 18-gauge steel cannula fitted through the middle of a double-hole, rubber stopper affixed to the top of the tube. Fractions (1.5 ml) were collected into 12×75 mm polystyrene tubes.

Basolateral and brush-border membrane fractions were identified by using marker enzymes, as described previously (Lash and Jones, 1982). Activities of GGT (EC 2.3.2.2) and $(\text{Na}^+ + \text{K}^+)\text{-stimulated ATPase}$ (EC 3.6.1.3) were used as markers for brush-border membrane and BLM vesicles, respectively. On the basis of the distribution of the activity of these markers, fractions comprising approximately 25% of the bottom of the Percoll gradient were used for the isolation of BLM vesicles. Pooled fractions were diluted approximately tenfold with buffer containing $500 \mu\text{M}$ α -ketoglutarate and were centrifuged at $100,000 g$ for 60 min to remove the Percoll and concentrate the membrane vesicles. The BLM pellet was resuspended in 1.5 ml of buffer, yielding a protein concentration of 2 to 4 mg/ml. Contamination of the BLM pellet with brush-border membranes was estimated to be $<5\%$, as judged by the activities of marker enzymes (Lash and Jones, 1982). Additionally, marker enzymes for cytoplasm, microsomes, lysosomes, and nuclei showed that the BLM pellet was minimally contaminated with these subcellular fractions.

Assays used to measure binding and transport of Hg^{2+} in BLM vesicles—Binding and transport of Hg^{2+} were assessed in 25-ml polypropylene Erlenmeyer flasks at 22°C . Basolateral membrane vesicles (1 mg protein/ml) were incubated with 0.03 ICi of $^{203}\text{HgCl}_2$ and various amounts of unlabeled Hg^{2+} in the form of either HgCl_2 or mercuric conjugates of Cys, GSH, or NAcCys. At indicated times, aliquots (0.5 ml) were filtered rapidly through nitrocellulose filters, having a pore size of $0.45\text{-}\mu\text{m}$, under vacuum. The filters were washed with standard sucrose buffer, and the radioactivity of the material retained on the filters was determined by gamma spectroscopy (see below). Binding of Hg^{2+} to the membranes was determined by incubation of membrane vesicles in a 1000 mOsmol/kg sucrose buffer, which reduces intravesicular volume to near zero (Murer and Kinne, 1980; Sachs *et al.*, 1980). Nonspecific association of radiolabel with the filters was typically $<5\%$ of total radioactivity in samples, and was subtracted from all measurements. Net transport was estimated by subtracting the amount of Hg^{2+} that was ostensibly bound to the plasma membranes (in a nonspecific manner) from the total amount of Hg^{2+} associated with the BLM vesicles.

Determination of content of Hg^{2+} in samples—The radioactivity of $^{203}\text{Hg}^{2+}$ in aliquots of BLM vesicles was determined by counting the samples in a Wallac 1282 CompuGamma CS deep-well gamma spectrometer (Wallac-PerkinElmer, Gaithersburg, MD) operating at a counting efficiency of 50% for $^{203}\text{Hg}^{2+}$. The actual content of Hg^{2+} in each sample was calculated by dividing the radioactivity of $^{203}\text{Hg}^{2+}$ in the sample (dpm) by the specific activity of $^{203}\text{Hg}^{2+}$ in prepared standards (dpm/nmol). The amount of Hg^{2+} in each sample was then expressed as nanomoles per milligram of protein.

Data analysis—Results are expressed as mean \pm SE of measurements from the indicated number of separate BLM vesicle preparations. Results are normalized to protein content, after measurement of protein with Coomassie blue G, according to the method of Read and Northcote (1981), using bovine serum albumin as a standard. Significant differences among selected mean values were first assessed by analysis of variance (one-way, two-way, three-way, or even four-way ANOVA, depending on the parameters being varied). Variables

included some or all of the following: (1) Hg^{2+} concentration, (2) surgical group (control, NPX), (3) presence or absence of Na^+ ions, and in some cases, (4) presence or absence of acivicin. When significant F-values were obtained with the analysis of variance, the Fisher's protected least significant difference *t*-test was performed to determine which means were significantly different from each other with two-tail probabilities of <0.05 considered significant.

RESULTS

Thiols, Na^+ Ions, and Compensatory Renal Growth Alter Binding of Hg^{2+} to BLM Vesicles

The disposition of Hg^{2+} in isolated plasma membrane vesicles from rat kidneys involves both transport across and binding to the membranes (Zalups and Lash, 1997). Moreover, binding accounts for a large component of the Hg^{2+} associated with the membrane vesicles. Furthermore, binding may also account for some of the differences in the handling of Hg^{2+} after compensatory renal cellular hypertrophy. Quantitation of binding under all incubation conditions was also necessary to determine the component of total Hg^{2+} associated with the membranes that is due to specific, carrier-mediated transport. Hence, assessment of binding was necessary from both a methodological standpoint, so that transport could be determined, and from a physiological standpoint, because the high affinity of Hg^{2+} for membrane sulfhydryl groups implies that binding occurs *in vivo* and is, therefore, a significant component of the renal disposition of Hg^{2+} . Accordingly, we quantified both binding and transport in renal BLM vesicles (isolated from both control and NPX rats) incubated with 1, 10, 20, 50, or 100 μM HgCl_2 (Fig. 1) or the same concentrations of $\text{Hg}-(\text{GSH})_2$, $\text{Hg}-(\text{Cys})_2$, or $\text{Hg}-(\text{NACys})_2$ (Fig. 2). Additionally, some vesicles were preincubated with 0.25 mM acivicin to assess the potential role of $\text{Hg}-(\text{GSH})_2$ -degradation on the binding and transport of Hg^{2+} .

In analyzing binding, two features were important: The specific amount of Hg^{2+} bound and the fraction of Hg^{2+} bound as compared to the total membrane-associated Hg^{2+} content. Data for the first feature are shown in Figures 1 and 2. Although data from the second feature are not shown, comparison of the binding data with those for transport presented below can be used to determine the fraction of binding of Hg^{2+} . Some key observations from the analysis of Hg^{2+} binding indicate that (1) the amount of binding of Hg^{2+} was markedly higher in BLM vesicles from control rats than those from NPX rats, regardless of the form of Hg^{2+} ; (2) the amount of binding of Hg^{2+} was markedly reduced by the presence of a thiol; (3) the fraction of Hg^{2+} bound to BLM vesicles from control rats decreased with increasing concentration of Hg^{2+} , whereas it generally increased in BLM vesicles from NPX rats with increasing concentrations of Hg^{2+} ; (4) the fraction of Hg^{2+} bound to BLM vesicles was generally lower when Na^+ ions were present than when they were absent; and (5) acivicin had little effect on either the amount or fraction of binding of Hg^{2+} when HgCl_2 or $\text{Hg}-(\text{GSH})_2$ were used as substrates. The most important implication of the lower level of binding and higher total association of Hg^{2+} in BLM vesicles from NPX rats relative to those from control rats, is that carrier-mediated transport plays a greater role in the renal disposition of Hg^{2+} in the former.

Time Course and Kinetics of Net Transport and Accumulation of Hg^{2+} -Thiol Conjugates into BLM Vesicles from Control and NPX Rats

It is clear from the results on total membrane-associated and membrane-bound Hg^{2+} that there were significant differences in the disposition of Hg^{2+} between the BLM vesicles from control rats and those from NPX rats. Thus, we determined the time courses and kinetics for the net uptake and intravesicular accumulation of Hg^{2+} in BLM vesicles from both surgical groups under various incubation conditions. Inasmuch as HgCl_2 is not a physiologically relevant transport form of Hg^{2+} *in vivo*, the remaining data focus on studies with Hg^{2+} -thiol conjugates as transportable substrates.

Net uptake of Hg^{2+} in BLM vesicles exposed to Hg^{2+} -thiol conjugates was determined over a 60-s time course at Hg^{2+} concentrations of 1, 10, 20, 50, and 100 μM . Time courses for the uptake of Hg^{2+} in BLM vesicles from control and NPX rats, when they were exposed to 20 μM Hg^{2+} , in the form of one of the three thiol-conjugates, in the presence and absence of Na^+ ions, are shown in Figure 3 as a sample of the data obtained. In all cases, and under all incubation conditions, the net amount of Hg^{2+} taken up increased with time up to 30 s. In the absence of Na^+ ions, the highest rates of net uptake and accumulation of Hg^{2+} occurred with HgCl_2 as substrate (data not shown). No effect of pretreatment with acivicin was detected in BLM vesicles from control rats in the absence of Na^+ ions or in BLM vesicles from NPX rats, in either the absence or presence of Na^+ ions. Among the BLM vesicles exposed to one of the Hg^{2+} -thiol conjugates, the rate of uptake of Hg^{2+} was faster in corresponding BLM vesicles exposed to $\text{Hg}-(\text{Cys})_2$ than in those exposed to either of the other two conjugates. At a concentration of 20 μM , net uptake and accumulation of Hg^{2+} , in the absence of Na^+ ions, was higher in BLM vesicles from NPX rats when $\text{Hg}-(\text{Cys})_2$ or $\text{Hg}-(\text{GSH})_2$ was used as a substrate. Net uptake and accumulation of Hg^{2+} , in the presence of Na^+ ions, was higher in BLM vesicles from NPX rats than in those from control rats when $\text{Hg}-(\text{GSH})_2$ was used as a substrate.

To assess more directly the effect of uninephrectomy and compensatory renal growth on net transport and accumulation of Hg^{2+} in BLM vesicles, uptake of Hg^{2+} was studied and compared in both the absence and the presence of Na^+ ions when the vesicles were exposed to extravesicular concentrations of one of the three Hg^{2+} -thiol conjugates, ranging from 1 μM to 100 μM . Rates of net uptake after 30 s of incubation were calculated for both uptake in the absence of Na^+ ions and for uptake calculated to be Na^+ -dependent (rate in presence of Na^+ ions – rate in absence of Na^+ ions) (Fig. 4). For $\text{Hg}-(\text{GSH})_2$ as the transport substrate, values shown for kinetics are those that were measured with BLM vesicles that were not pretreated with acivicin, as no significant effects of acivicin pretreatment were observed.

Concentration-dependence profiles of both Na^+ -independent and Na^+ -dependent uptake of each of the three Hg^{2+} -thiol conjugates exhibited Michaelis-Menten kinetics. In the absence of Na^+ ions, BLM vesicles from NPX rats exhibited significantly higher rates of uptake at most concentrations of $\text{Hg}-(\text{GSH})_2$ and $\text{Hg}-(\text{Cys})_2$ tested, but only at 1 μM $\text{Hg}-(\text{NACys})_2$. In contrast, rates of Na^+ -dependent uptake of $\text{Hg}-(\text{GSH})_2$ and $\text{Hg}-(\text{Cys})_2$ in BLM vesicles from NPX rats were significantly higher than those in BLM vesicles from control rats at all concentrations tested; the same was true for $\text{Hg}-(\text{NACys})_2$ at the three lowest concentrations (*i.e.*, 1, 10, 20 μM) tested. Depending on exposure conditions, the magnitude of Hg^{2+} accumulation differed. The order of the magnitude of uptake in the absence of Na^+ in BLM vesicles from either control or NPX rats was as follows: $\text{Hg}-(\text{Cys})_2 > \text{Hg}-(\text{NACys})_2 \gg \text{Hg}-(\text{GSH})_2$; for BLM vesicles from either control or NPX rats, the order of Na^+ -dependent uptake was $\text{Hg}-(\text{Cys})_2 = \text{Hg}-(\text{GSH})_2 > \text{Hg}-(\text{NACys})_2$.

Based on the Michaelis-Menten plots (*cf.* Fig. 4), Eadie-Hofstee plots were constructed and kinetic parameters were derived for each Hg^{2+} -thiol conjugate and each surgical group, for both Na^+ -independent and Na^+ -dependent uptake rates (Figs. 5–7, Table 1). In all but one case, the Eadie-Hofstee plots were easily resolvable into two components, suggesting that at least two separate transporter proteins participated in the uptake process.

When $\text{Hg}-(\text{GSH})_2$ was used as the transport substrate, no significant differences in K_m or V_{max} values were apparent between BLM vesicles from control and NPX rats for either of the two transporter components for Na^+ -independent uptake (Fig. 5, Table 1). By contrast, K_m values for the high- and low-affinity transport processes for Na^+ -dependent uptake were approximately fourfold and twofold higher, respectively, in BLM vesicles from control rats than in BLM vesicles from NPX rats.

When Hg-(Cys)₂ was used as the transport substrate, there were no significant differences in the kinetic parameters for Na⁺-independent uptake between BLM vesicles from control and NPX rats (Fig. 6, Table 1). This pattern is similar to that when Hg-(GSH)₂ was used as the transport substrate. For Na⁺-dependent uptake of Hg-(Cys)₂, however, the Eadie-Hofstee plots indicate marked differences in BLM vesicles from control and NPX rats. Basolateral membrane vesicles from control rats exhibited only a single, discernible transport process, whereas those from NPX rats exhibited the typical pattern of a high-affinity, low-capacity and low-affinity, high-capacity process. The K_m value for the single process in BLM vesicles from control rats was approximately fourfold higher than the K_m value for the high-affinity, low-capacity process in BLM vesicles from NPX rats.

Eadie-Hofstee plots for the Na⁺-independent transport of Hg-(NACys)₂ also exhibited two discernible processes (Fig. 7, Table 1). While V_{max} values for both processes were similar in BLM vesicles from the two surgical groups and K_m values for the low-affinity, high-capacity process were similar as well, the K_m value for the high-affinity, low-capacity process was actually fourfold higher in BLM vesicles from NPX rats. This one difference contrasts with results when the other Hg²⁺-thiol conjugates were used as substrates. For Na⁺-dependent transport, kinetic parameters for the high-affinity, low-capacity process were similar in BLM vesicles from the two surgical groups, as were the V_{max} values for the low-affinity, high-capacity process. The only difference was that the K_m value for the low-affinity, high-capacity process was approximately sixfold higher in BLM vesicles from control rats as in those from NPX rats.

Organic Anion and Amino Acid Transporters Participate in Hg²⁺-Thiol Conjugate Transport into BLM Vesicles, and Are Altered Selectively by Compensatory Renal Growth

To assess the effects of uninephrectomy and compensatory renal growth on the transport of Hg²⁺-thiol conjugates by specific transport systems, net uptake of 20 μM Hg²⁺-thiol conjugate was measured over a 60-s time course in the presence of 500 μM of various characteristic carrier substrates. In an attempt to present the data more clearly, only values for net accumulation of Hg²⁺ at 30 s are presented. Binding of Hg²⁺ for each of the three Hg²⁺-thiol conjugates to BLM vesicles was not affected by the presence of any of the characteristic carrier substrates (data not shown).

Net Na⁺-dependent accumulation of Hg-(GSH)₂ in BLM vesicles from control rat kidneys was significantly inhibited by PAH, glutarate, and L-γ-glutamyl-L-glutamate, implicating the function of OAT1 and/or OAT3 and SDCT2 (Fig. 8). A small degree of additional inhibition was observed when the three competing substrates were combined, suggesting that these and any additional carriers for GSH conjugates and other γ-glutamyl compounds are functioning simultaneously in the transport of Hg-(GSH)₂. The only significant effect of acivicin pretreatment was observed when incubations were performed with all three inhibitors simultaneously. Similar inhibition of net accumulation of Hg-(GSH)₂ by PAH, glutarate, and L-γ-glutamyl-L-glutamate was observed in BLM vesicles from NPX rat kidneys, with no significant effect of acivicin pretreatment being observed. The degree of inhibition of Hg-(GSH)₂ transport was greater in BLM vesicles from the sole kidney of NPX rats than in two kidneys from control rats.

Net Na⁺-dependent accumulation of Hg-(Cys)₂ in BLM vesicles from control rat kidneys was significantly inhibited by *p*-aminohippurate (PAH), glutarate, L-alanine, and L-lysine, implicating the activity of OAT1 and/or OAT3, SDCT2, system ASC, and DBAT (Fig. 9). L-Phenylalanine had no effect on Na⁺-independent Hg-(Cys)₂ accumulation, suggesting that system L does not function in Hg-(Cys)₂ transport. Similar results were obtained in incubations of Hg-(Cys)₂ with BLM vesicles from NPX rat kidney, although the degree of inhibition by

each characteristic substrate appeared to be somewhat less than that in BLM vesicles from control rat kidneys.

Net Na⁺-dependent accumulation of Hg-(NACys)₂ in BLM vesicles from control rat kidneys was significantly inhibited by PAH and L-alanine (Fig. 10), suggesting that OAT1 and/or OAT3 and the amino acid transporter system ASC are involved in the transport of Hg-(NACys)₂. In renal BLM vesicles from NPX rats, a somewhat different pattern was observed, with significant inhibition occurring with PAH and L-phenylalanine. However, L-phenylalanine did not inhibit Na⁺-independent Hg-(NACys)₂ accumulation. Taken together, these findings implicate a role for OAT1 and/or OAT3, but not the amino acid transporter system L, in the transport of Hg-(NACys)₂.

DISCUSSION

In the present study, we sought to determine how renal accumulation and disposition of Hg²⁺ are altered as a result of compensatory renal growth and what transport processes may be associated with the changes. We chose isolated BLM vesicles as the experimental model for several reasons. First, we have many years of experience with this biological model (Lash and Jones, 1982, 1985a; Zalups and Lash, 1997; Zalups and Minor, 1995). Second, the nature of this model allows us to manipulate and precisely define the incubation environment, thereby enabling us to discriminate clearly between Na⁺-dependent and Na⁺-independent processes and between binding to the plasma membrane and actual transport into the intravesicular space. Third, use of this model eliminates most of the confounding metabolic processes that may occur within the cell and may obscure the results. Finally, use of BLM vesicles obtained from normal rat kidneys and from the remnant kidney of a rat that has undergone uninephrectomy and compensatory renal growth allows us to directly assess the effects of compensatory renal growth on binding and transport.

Analysis of kinetics of net uptake and intravesicular accumulation of Hg²⁺-thiol conjugates in BLM vesicles from kidney(s) of control and NPX rats showed differences in both K_m and V_{max} values for Na⁺-independent and Na⁺-dependent processes. With Hg-(GSH)₂ as a substrate, V_{max} values for both Na⁺-dependent systems discriminated by Eadie-Hofstee analysis were 25% to 35% higher in BLM vesicles from the remnant kidney of NPX rats. The low-affinity, high-capacity system for Na⁺-independent transport was also 25% higher in BLM vesicles from the NPX rat kidney than in those from control rat kidneys. Larger differences were observed in K_m values, with those for Na⁺-dependent transport being 78% and 52% lower for the two systems in BLM vesicles from the NPX rat kidney. This decrease in K_m is likely due to an increase in transport sites that result from compensatory cellular hypertrophy. More complex changes were observed in the transport of Hg-(Cys)₂. Although only modest changes were observed in kinetic parameters of Na⁺-independent transport, markedly different kinetics for Na⁺-dependent uptake were observed in BLM vesicles from kidney(s) of the two surgical groups. Eadie-Hofstee analysis resolved only one transport system in BLM vesicles from the kidneys of control rats but two transport systems in BLM vesicles from the remnant kidney of NPX rats. With Hg-(NACys)₂ as a substrate, modest differences were observed in the kinetic parameters for the two transport systems under Na⁺-independent or Na⁺-dependent conditions. As noted above, however, little or no change in transport properties, particularly V_{max} values, actually indicates an increase in net rates of transport because of the increase in membrane protein content resulting from compensatory growth.

Competition experiments demonstrated that OAT1 and/or OAT3 (PAH- and glutarate-inhibitable), possibly SDCT2 (glutarate-inhibitable), system ASC (L-alanine-inhibitable), and DBAT (L-lysine-inhibitable) all play a role in the net uptake and accumulation of Hg-(Cys)₂ in renal BLM vesicles from both control and NPX rats. It appears that when Hg-(NACys)₂ is

presented to the BLM, OAT1 and/or OAT3 and system ASC participate in the net uptake and accumulation of Hg^{2+} . When $\text{Hg}-(\text{GSH})_2$ is presented to the BLM, it appears that both OAT1 and/or OAT3, and possibly SDCT2, are involved in the net uptake and accumulation of Hg^{2+} . These findings are consistent with previous results demonstrating a role for PAH- or probenecid-inhibitable transport in the uptake of organic conjugates of GSH (Lash and Jones, 1985a). $\text{L-}\gamma$ -Glutamyl-L-glutamate was also a potent inhibitor of $\text{Hg}-(\text{GSH})_2$ transport, providing additional evidence that the $\text{Hg}-(\text{GSH})_2$ conjugate is handled similarly at the renal BLM as are other GSH conjugates. Inasmuch as glutarate is a substrate for OAT1, OAT3, and SDCT2 at high concentrations, any conclusion about the specific role of SDCT2 in $\text{Hg}-(\text{Cys})_2$ or $\text{Hg}-(\text{GSH})_2$ transport will require further validation. Additional competition studies with more carrier-selective substrates and inhibitors can help provide further information about the function of each carrier in Hg^{2+} -thiol conjugate transport.

As far as a role or requirement for GGT activity in the net uptake and accumulation of $\text{Hg}-(\text{GSH})_2$ is concerned, experiments performed with competitive inhibitors were done with 20 μM $\text{Hg}-(\text{GSH})_2$ in both untreated and acivicin-pretreated vesicles. It is not surprising that no effects of acivicin-pretreatment were observed, because acivicin only appeared to have a modest effect at the highest concentrations of $\text{Hg}-(\text{GSH})_2$ used (*i.e.*, $\geq 50 \mu\text{M}$) (cf. Fig. 2). The absence of a significant effect of acivicin on $\text{Hg}-(\text{GSH})_2$ uptake and accumulation, therefore, indicates that while a small portion of the Hg^{2+} that accumulates in renal cells incubated with $\text{Hg}-(\text{GSH})_2$ is transported as $\text{Hg}-(\text{Cys})_2$ and/or possibly as a mercuric conjugate of L-cysteinylglycine, most is transported as intact $\text{Hg}-(\text{GSH})_2$. Hence, we conclude that GGT activity is not required for the uptake of Hg^{2+} in BLM vesicles when $\text{Hg}-(\text{GSH})_2$ is used as the transport substrate.

Our findings support the overall hypothesis that the increased susceptibility of NPX rats to the nephrotoxic effects of Hg^{2+} relative to that of rats with two normal kidneys is associated with increased renal uptake and accumulation of Hg^{2+} . Moreover, the most novel aspect of our findings is that we can associate the increased transport of Hg^{2+} with effects on activities of specific carrier proteins. More specifically, our findings implicate specific transport systems at the BLM and increases in the level of transport and accumulation of specific molecular species of Hg^{2+} that occur in association with compensatory renal growth. The identity of the carrier proteins involved in this compensatory response depends on the transport form of Hg^{2+} , differing if Hg^{2+} is presented as $\text{Hg}-(\text{Cys})_2$, $\text{Hg}-(\text{GSH})_2$, or $\text{Hg}-(\text{NAcCys})_2$. It is significant that the changes occurring after uninephrectomy and compensatory renal growth are not simply representative of an overall increase in transport activity. Thus, while there are some increases in total membrane-associated Hg^{2+} (again, dependent on the form of Hg^{2+}), the most prominent effect is a significant redistribution of accumulated Hg^{2+} between that which is membrane-bound and that which is transported (cf. Figs. 1 and 2). Additionally, variations in response were observed in the absence and presence of Na^+ ions. Although the presence of Na^+ ions only slightly decreased the fraction of membrane-bound Hg^{2+} (possibly owing to a simple charge effect), altered function of specific, Na^+ -coupled carrier proteins was important in the enhanced uptake and accumulation of Hg^{2+} or Hg^{2+} -thiol conjugates.

Our present findings pertaining to the binding of Hg^{2+} to the BLM confirm and extend those of an earlier study (Zalups and Lash, 1997). In general, there was a markedly lower proportion of membrane binding of Hg^{2+} , but a similar or higher amount of total membrane-associated Hg^{2+} in the renal BLM vesicles from NPX rats than in those from control rats. This pattern of binding leads us to the overall conclusion that transport into the intravesicular space, as distinguished from other forms of membrane association (primarily binding), is increased in renal BLM vesicles after uninephrectomy and compensatory renal growth. Additional support for this conclusion was obtained by quantifying net uptake and intravesicular accumulation of Hg^{2+} (cf. Figs. 3–7). The form and concentration of Hg^{2+} , the presence or absence of Na^+ ions,

and whether renal BLM vesicles were derived from control or NPX rats, clearly made a difference in the extent of uptake and accumulation. Under many conditions, the largest amount of Hg^{2+} accumulation was detected with HgCl_2 as substrate, although this is not believed to be a physiological transport form of Hg^{2+} . Under other conditions, the largest amount of Hg^{2+} accumulation was detected when $\text{Hg}-(\text{Cys})_2$ or $\text{Hg}-(\text{NAcCys})_2$ were used as transportable substrates. For most conditions, Hg^{2+} accumulation with $\text{Hg}-(\text{Cys})_2$ was greater than that with $\text{Hg}-(\text{NAcCys})_2$. In all cases, however, Hg^{2+} accumulation with $\text{Hg}-(\text{GSH})_2$ was less than that with $\text{Hg}-(\text{Cys})_2$. Because Cys and its various forms are present at higher concentrations than GSH and its various forms in rat plasma (Lash and Jones, 1985b), $\text{Hg}-(\text{Cys})_2$ is probably a more important physiological transport form of Hg^{2+} than $\text{Hg}-(\text{GSH})_2$.

There are two additional issues that arise from these studies: The first issue pertains to the mechanism of increased carrier activity after compensatory hypertrophy. One possibility is an increase in carrier protein expression. An alternative mechanism would involve post-translational modifications, such as phosphorylation. For example, the OATs are known to be regulated by various hormones and protein kinases (Wright and Dantzler, 2004). The second issue is that of changes in luminal transport processes that might influence renal accumulation of Hg^{2+} . We have performed studies similar to those presented here, but using isolated brush border membrane (BBM) vesicles (Lash, L. H., Hueni, S. E., Putt, D. A., and Zalups, R. K., manuscript in preparation). This is critical for putting the BLM transport results into the context of events that occur in the intact proximal tubule.

In conclusion, the present study demonstrates that compensatory renal growth is indeed associated with increased transport of Hg^{2+} across the BLM, and that specific organic anion and amino acid carriers are involved in the increased transport of Hg^{2+} -thiol conjugates. We also show that both binding and transport are important determinants in the renal cellular accumulation of Hg^{2+} . Our results illustrate the complexities of the biochemical and molecular changes that proximal tubular cells of remnant renal tissue undergo following compensatory renal growth.

Acknowledgements

This work was funded by National Institute of Environmental Health Sciences grants R01-ES05157, ES05980, and ES11288 (to R.K.Z.) and National Institute of Diabetes and Digestive and Kidney Diseases grant R01-DK40725 (to L.H.L.).

References

- Aslamkhan AG, Han YH, Yang XP, Zalups RK, Pritchard JB. Human renal organic anion transporter 1-dependent uptake and toxicity of mercuric-thiol conjugates in Madin-Darby canine kidney cells. *Mol Pharmacol* 2003;63:590–596. [PubMed: 12606766]
- Barfuss DW, Robinson MK, Zalups RK. Inorganic mercury transport in the proximal tubule of the rabbit. *J Am Soc Nephrol* 1990;1:910–917. [PubMed: 2103850]
- Cannon VT, Barfuss DW, Zalups RK. Molecular homology (“mimicry”) and the mechanisms involved in the luminal uptake of inorganic mercury in the proximal tubule of the rabbit. *J Am Soc Nephrol* 2000;11:394–402. [PubMed: 10703663]
- Houser MT, Berndt WO. The effect of unilateral nephrectomy on the nephrotoxicity of mercuric chloride in the rat. *Toxicol Appl Pharmacol* 1986;83:506–515. [PubMed: 3705072]
- Houser MT, Berndt WO. Unilateral nephrectomy in the rat: Effects on mercury handling and renal cortical subcellular distribution. *Toxicol Appl Pharmacol* 1988;93:187–194. [PubMed: 3358258]
- Lash LH, Jones DP. Localization of the membrane-associated thiol oxidase of rat kidney to the basal-lateral plasma membrane. *Biochem J* 1982;203:371–376. [PubMed: 6126181]
- Lash LH, Jones DP. Uptake of the glutathione conjugate S-(1,2-dichlorovinyl)- glutathione by renal basal-lateral membrane vesicles and isolated kidney cells. *Mol Pharmacol* 1985a;28:278–282. [PubMed: 3839897]

- Lash LH, Jones DP. Distribution of oxidized and reduced forms of glutathione and cyst(e)ine in rat plasma. *Arch Biochem Biophys* 1985b;240:583–592. [PubMed: 4026295]
- Lash LH, Zalups RK. Mercuric chloride-induced cytotoxicity and compensatory hypertrophy in rat kidney proximal tubular cells. *J Pharmacol Exp Ther* 1992;261:819–829. [PubMed: 1578387]
- Lash LH, Putt DA, Zalups RK. Role of extracellular thiols in uptake and distribution of inorganic mercury in rat renal proximal and distal tubular cells. *J Pharmacol Exp Ther* 1998;285:1039–1050. [PubMed: 9618406]
- Lash LH, Putt DA, Zalups RK. Influence of exogenous thiols on mercury-induced cellular injury in isolated renal proximal tubular and distal tubular cells from normal and uninephrectomized rats. *J Pharmacol Exp Ther* 1999;291:492–502. [PubMed: 10525063]
- Murer H, Kinne R. The use of isolated membrane vesicles to study epithelial transport processes. *J Membr Biol* 1980;55:81–95. [PubMed: 6997489]
- Read SM, Northcote DH. Minimization of variation in the response to different proteins of the Coomassie blue G dye-binding assay for protein. *Anal Biochem* 1981;116:53–64. [PubMed: 7304986]
- Sachs G, Jackson RL, Rabon EC. Use of plasma membrane vesicles. *Am J Physiol* 1980;238:G151–G164. [PubMed: 6245586]
- Scalera V, Huang YK, Hildmann B, Murer H. A simple isolation method for basal-lateral plasma membranes from rat kidney cortex. *Membr Biochem* 1981;4:49–61. [PubMed: 6261079]
- Tanaka-Kagawa T, Naganuma A, Imura N. Tubular secretion and reabsorption of mercury compounds in mouse kidney. *J Pharmacol Exp Ther* 1993;264:776–782. [PubMed: 8094752]
- Wright SH, Dantzer WH. Molecular and cellular physiology of renal organic cation and anion transport. *Physiol Rev* 2004;84:987–1049. [PubMed: 15269342]
- Zalups RK. Autometallographic localization of inorganic mercury in the kidneys of rats: Effect of unilateral nephrectomy and compensatory renal growth. *Exp Mol Pathol* 1991a;54:10–21. [PubMed: 1995316]
- Zalups RK. Method for studying the *in vivo* accumulation of inorganic mercury in segments of the nephron in the kidneys of rats treatment with mercuric chloride. *J Pharmacol Methods* 1991b;26:89–104. [PubMed: 1943126]
- Zalups RK. Organic anion transport and action of γ -glutamyl transpeptidase in kidney linked mechanistically to renal tubular uptake of inorganic mercury. *Toxicol Appl Pharmacol* 1995;132:289–298. [PubMed: 7785056]
- Zalups RK. Reductions in renal mass and the nephropathy induced by mercury. *Toxicol Appl Pharmacol* 1997;143:366–379. [PubMed: 9144453]
- Zalups RK. Basolateral uptake of mercuric conjugates of N-acetylcysteine and cysteine in the kidney involves the organic anion transport system. *J Toxicol Environ Health* 1998a;55:13–29.
- Zalups RK. Basolateral uptake of inorganic mercury in the kidney. *Toxicol Appl Pharmacol* 1998b; 151:192–199. [PubMed: 9705903]
- Zalups RK. Molecular interactions with mercury in the kidney. *Pharmacol Rev* 2000;52:113–143. [PubMed: 10699157]
- Zalups RK, Ahmad S. Homocysteine and the renal epithelial transport and toxicity of inorganic mercury: Role of basolateral transporter OAT1. *J Am Soc Nephrol* 2004;15:2023–2031. [PubMed: 15284288]
- Zalups RK, Barfuss DW. Accumulation of inorganic mercury along the renal proximal tubule of the rabbit. *Toxicol Appl Pharmacol* 1990;106:245–253. [PubMed: 2256114]
- Zalups RK, Barfuss DW. Renal disposition of mercury in rats after intravenous injection of inorganic mercury and cysteine. *J Toxicol Environ Health* 1995a;44:401–413. [PubMed: 7723073]
- Zalups RK, Barfuss DW. Pretreatment with p-aminohippurate inhibits the renal uptake and accumulation of injected inorganic mercury in the rat. *Toxicology* 1995b;103:23–35. [PubMed: 8525487]
- Zalups RK, Barfuss DW. Accumulation and handling of inorganic mercury in the kidney after coadministration with glutathione. *J Toxicol Environ Health* 1995c;44:385–399. [PubMed: 7723072]
- Zalups RK, Barfuss DW. Participation of mercuric conjugates of cysteine, homocysteine, and N-acetylcysteine in mechanisms involved in the renal tubular uptake of inorganic mercury. *J Am Soc Nephrol* 1998a;9:551–561. [PubMed: 9555656]

- Zalups RK, Barfuss DW. Small aliphatic dicarboxylic acids inhibit renal uptake of administered mercury. *Toxicol Appl Pharmacol* 1998b;148:183–193. [PubMed: 9465278]
- Zalups RK, Barfuss DW. Renal organic anion transport system: A mechanism for the basolateral uptake of mercury-thiol conjugates along the Pars Recta of the proximal tubule. *Toxicol Appl Pharmacol* 2002;182:234–243. [PubMed: 12183103]
- Zalups RK, Diamond GL. Mercuric chloride-induced nephrotoxicity in the rat following unilateral nephrectomy and compensatory renal growth. *Virchows Arch B* 1987;53:336–346. [PubMed: 2891217]
- Zalups RK, Lash LH. Effects of uninephrectomy and mercuric chloride on renal glutathione homeostasis. *J Pharmacol Exp Ther* 1990;254:962–970. [PubMed: 2395124]
- Zalups RK, Lash LH. Advances in understanding the renal transport and toxicity of mercury. *J Toxicol Environ Health* 1994;42:1–44. [PubMed: 8169994]
- Zalups RK, Lash LH. Binding of mercury in renal brush-border and basolateral membrane-vesicles: Implication of a cysteine conjugate of mercury involved in the luminal uptake of inorganic mercury in the kidney. *Biochem Pharmacol* 1997;53:1889–1900. [PubMed: 9256164]
- Zalups RK, Minor KH. Luminal and basolateral mechanisms involved in the renal tubular uptake of inorganic mercury. *J Toxicol Environ Health* 1995;46:73–100. [PubMed: 7666495]
- Zalups RK, Aslamkhan AG, Ahmad S. Human organic anion transporter 1 mediates cellular uptake of cysteine-S conjugates of inorganic mercury. *Kidney Int* 2004;66:251–261. [PubMed: 15200431]
- Zalups RK, Klotzbach JM, Diamond GL. Enhanced accumulation of injected inorganic mercury in renal outer medulla after unilateral nephrectomy. *Toxicol Appl Pharmacol* 1987;89:226–236. [PubMed: 3603559]

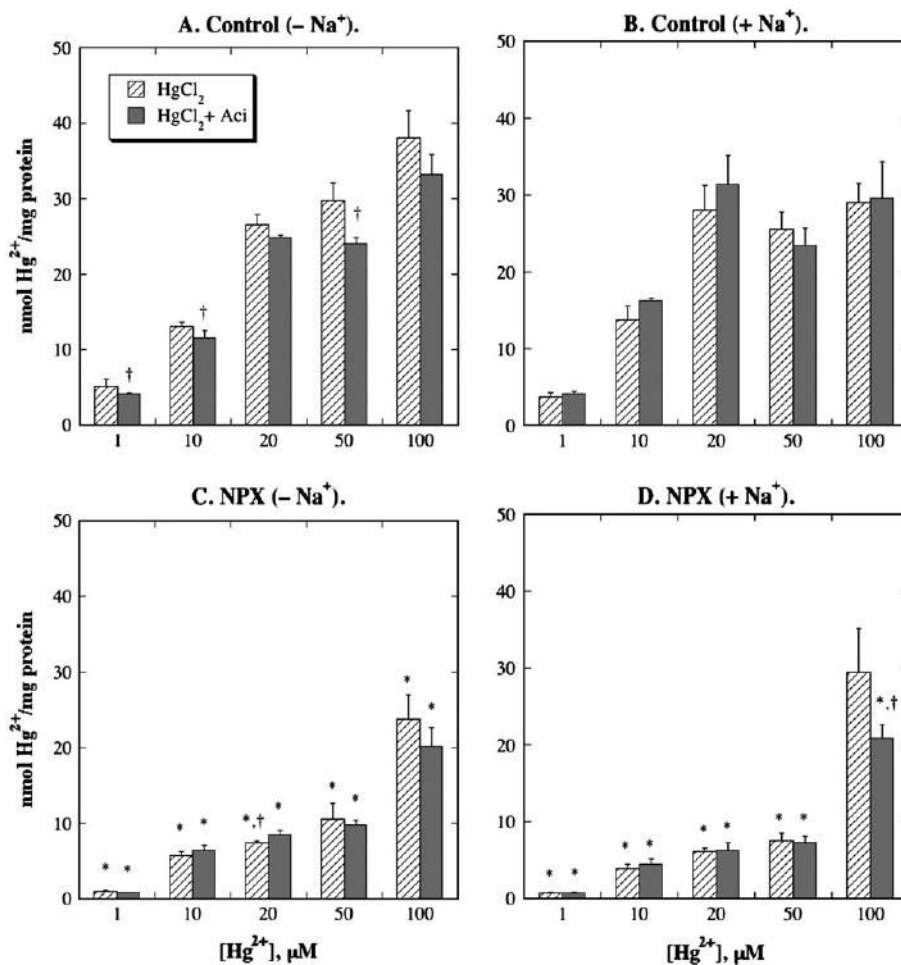


FIG. 1.

Binding of Hg^{2+} , with HgCl_2 as substrate, to basolateral membrane (BLM) vesicles from control and NPX rat kidney(s). Total membrane-associated Hg^{2+} was measured by incubating BLM vesicles with 1, 10, 20, 50, or 100 μM Hg^{2+} as the chloride salt and $^{203}\text{Hg}^{2+}$, for up to 60 s in standard, 300 mOsmol/kg buffered sucrose solution. Binding of Hg^{2+} was determined by incubating BLM vesicles as above for 60 s in a buffered sucrose solution with an osmolarity of 1000 mOsmol/kg. Where indicated, samples were preincubated for 15 min with 0.25 mM acivicin. Results are expressed as $\text{nmol Hg}^{2+}/\text{mg protein}$ and are means \pm SE of measurements from separate membrane vesicle preparations from three control and three NPX rats each.

*Statistically significant difference ($p < 0.05$) from corresponding control sample.

†Statistically significant difference ($p < 0.05$) from corresponding sample without acivicin.

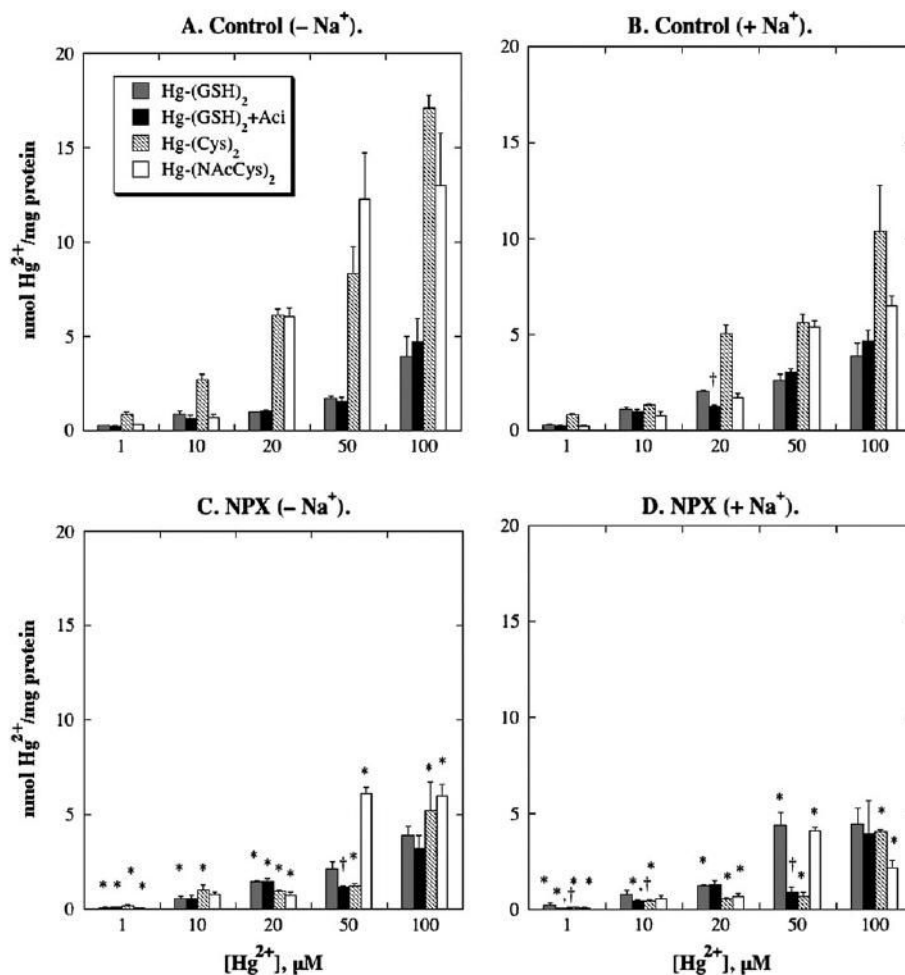


FIG. 2. Binding of Hg²⁺-thiol conjugates to BLM vesicles from control and NPX rat kidney(s). Total membrane-associated Hg²⁺ was measured by incubating BLM vesicles with 1, 10, 20, 50, or 100 μM Hg²⁺ in combination with a threefold molar excess of GSH, L-cysteine (Cys), or N-acetyl-L-cysteine (NACys), and ²⁰³Hg²⁺, for up to 60 s in standard, 300 mOsmol/kg buffered sucrose solution. Binding of Hg²⁺ was determined by incubating BLM vesicles as above for 60 s in a buffered sucrose solution with an osmolarity of 1000 mOsmol/kg. Where indicated, samples were preincubated for 15 min with 0.25 mM acivicin. Results are expressed as nmol Hg²⁺/mg protein and are means ± SE of measurements from separate membrane vesicle preparations from three control and three NPX rats each. *Statistically significant difference ($p < 0.05$) from corresponding control sample. †Statistically significant difference ($p < 0.05$) from corresponding sample without acivicin.

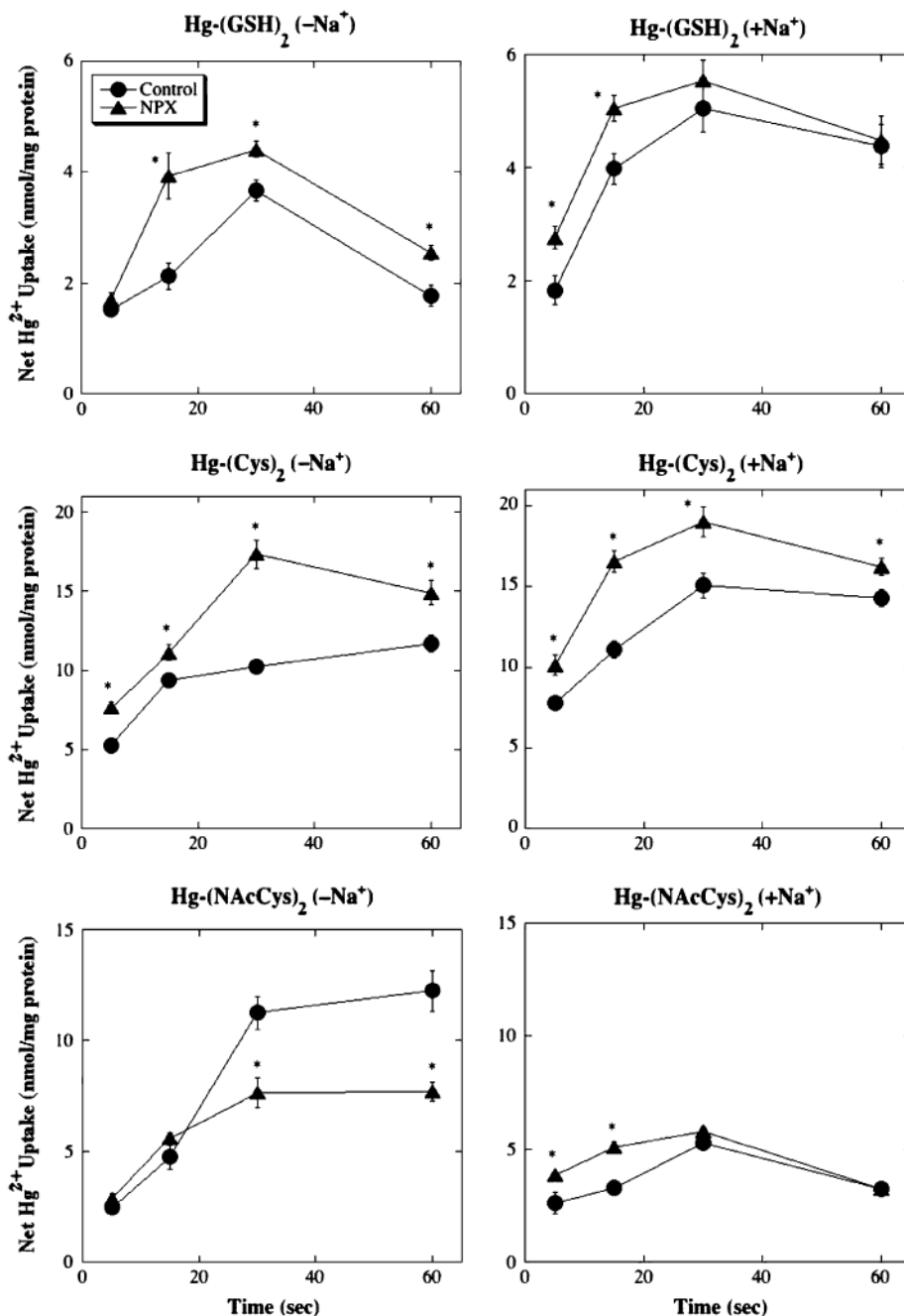
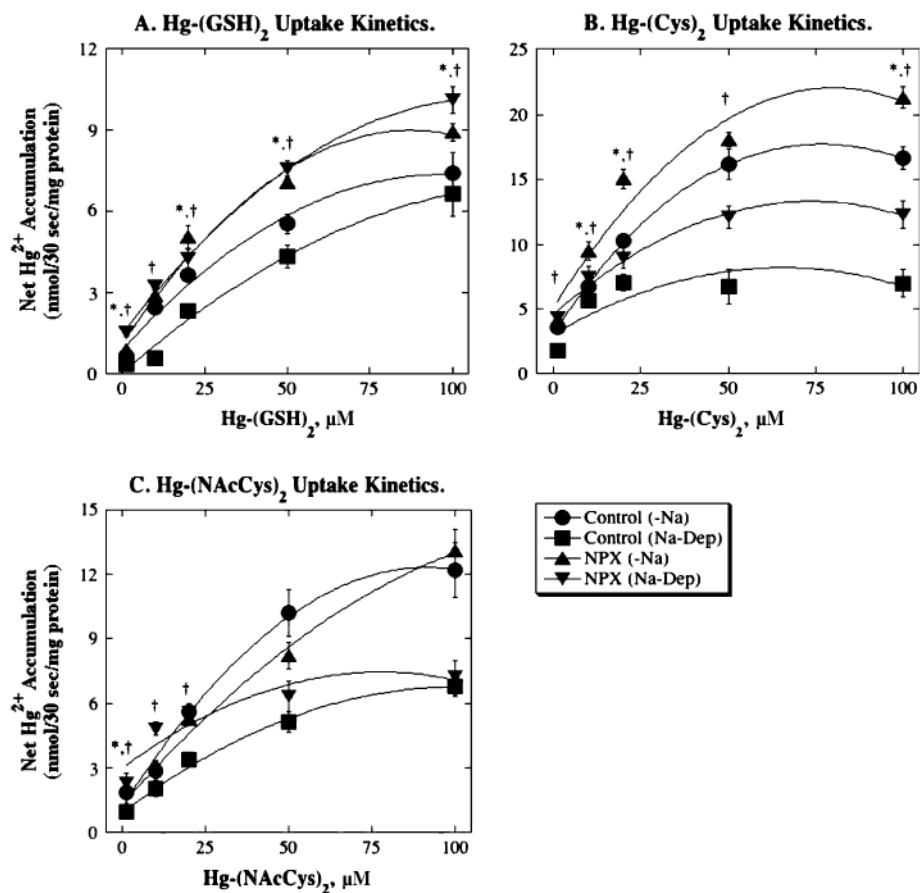


FIG. 3.

Time courses for net uptake of 20 μM Hg^{2+} -thiol conjugates in BLM vesicles from control and NPX rat kidney(s). Net uptake of 20 μM of either $\text{Hg}-(\text{GSH})_2$, $\text{Hg}-(\text{Cys})_2$, or $\text{Hg}-(\text{NACys})_2$ in BLM vesicles was determined by incubating with medium containing $^{203}\text{Hg}^{2+}$, in the presence and absence of Na^+ ions. Binding was subtracted from total intravesicular contents to give net uptake. Results are expressed as nmol Hg^{2+} /mg protein and are means \pm SE of measurements from separate membrane vesicle preparations from three control and three NPX rats. *Significantly different ($p < 0.05$) from corresponding BLM vesicles from control rat kidneys.

**FIG. 4.**

Michaelis-Menten kinetics of Hg²⁺-thiol conjugate transport in BLM vesicles from control and NPX rat kidney(s). Values for net accumulation of Hg²⁺ after 30-s incubations with 1, 10, 20, 50, or 100 μM Hg-(GSH)₂, Hg-(Cys)₂, or Hg-(NAcCys)₂ are plotted. Results are means ± SE of measurements from separate membrane vesicle preparations from three control and three NPX rats. Curves were obtained by polynomial regression analysis. *Significant difference ($p < 0.05$) between values in BLM vesicles from control and NPX rats for uptake -Na⁺. †Significant difference ($p < 0.05$) between values in BLM vesicles from control and NPX rats for Na⁺-dependent uptake. Regression curves and correlation coefficients are as follows: Panel A: **Control (-Na⁺):** $Y = 0.0284 + 0.10725X - 0.00041X^2$, $r^2 = 0.988$; **Control (Na⁺-Dep.):** $Y = 0.8844 + 0.13423X - 0.00070X^2$, $r^2 = 0.984$; **NPX (-Na⁺):** $Y = 1.1086 + 0.18049X - 0.00103X^2$, $r^2 = 0.976$; **NPX (Na⁺-Dep.):** $Y = 1.4933 + 0.15653X - 0.000705X^2$, $r^2 = 0.998$. Panel B: **Control (-Na⁺):** $Y = 3.0647 + 0.42X - 0.00344X^2$, $r^2 = 0.999$; **Control (Na⁺-Dep.):** $Y = 3.0609 + 0.1576X - 0.00120X^2$, $r^2 = 0.678$; **NPX (-Na⁺):** $Y = 5.158 + 0.425X - 0.00266X^2$, $r^2 = 0.940$; **NPX (Na⁺-Dep.):** $Y = 4.619 + 0.237X - 0.00161X^2$, $r^2 = 0.981$. Panel C: **Control (-Na⁺):** $Y = 1.1851 + 0.2437X - 0.00133X^2$, $r^2 = 0.992$; **Control (Na⁺-Dep.):** $Y = 0.9464 + 0.1162X - 0.000581X^2$, $r^2 = 0.993$; **NPX (-Na⁺):** $Y = 1.307 + 0.1756X - 0.000585X^2$, $r^2 = 0.991$; **NPX (Na⁺-Dep.):** $Y = 3.008 + 0.1144X - 0.000736X^2$, $r^2 = 0.864$.

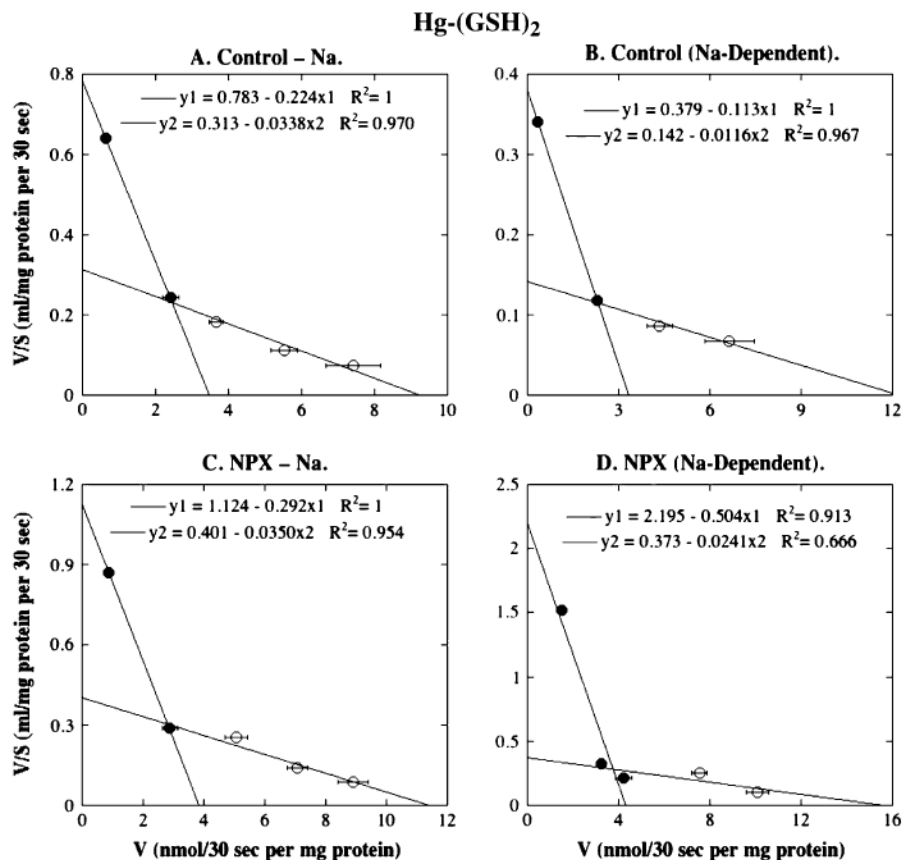
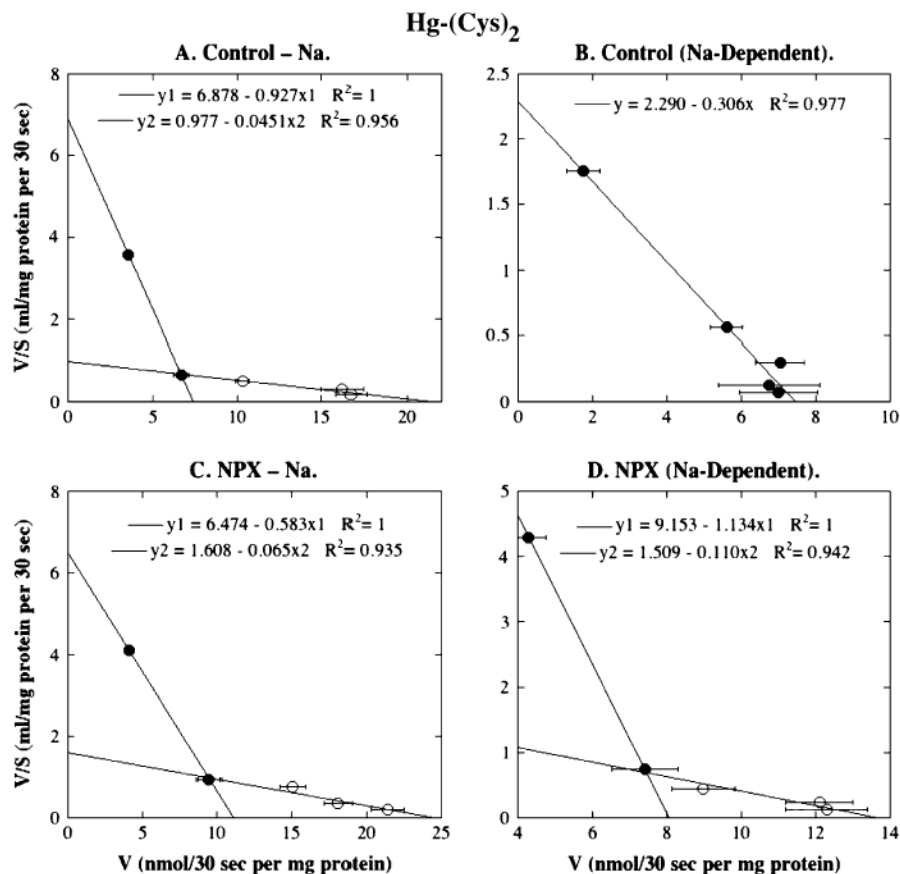


FIG. 5. Eadie-Hofstee plots for Hg-(GSH)₂ transport in BLM vesicles from control and NPX rat kidney (s). Initial rates of Hg-(GSH)₂ transport derived from Figure 3A for Na⁺-independent and Na⁺-dependent uptake were linearized by Eadie-Hofstee analysis and represent means ± SE of measurements from separate membrane vesicle preparations from three control and three NPX rats. Where not visible, error bars were within the size of the data point. Filled and open symbols represent data points from different ranges that were selected to provide the best fit for linear regression.

**FIG. 6.**

Eadie-Hofstee plots for Hg-(Cys)₂ transport in BLM vesicles from control and NPX rat kidney (s). Initial rates of Hg-(Cys)₂ transport derived from Figure 3B for Na⁺-independent and Na⁺-dependent uptake were linearized by Eadie-Hofstee analysis and represent means ± SE of measurements from separate membrane vesicle preparations from three control and three NPX rats. Where not visible, error bars were within the size of the data point. Filled and open symbols represent data points from different ranges that were selected to provide the best fit for linear regression.

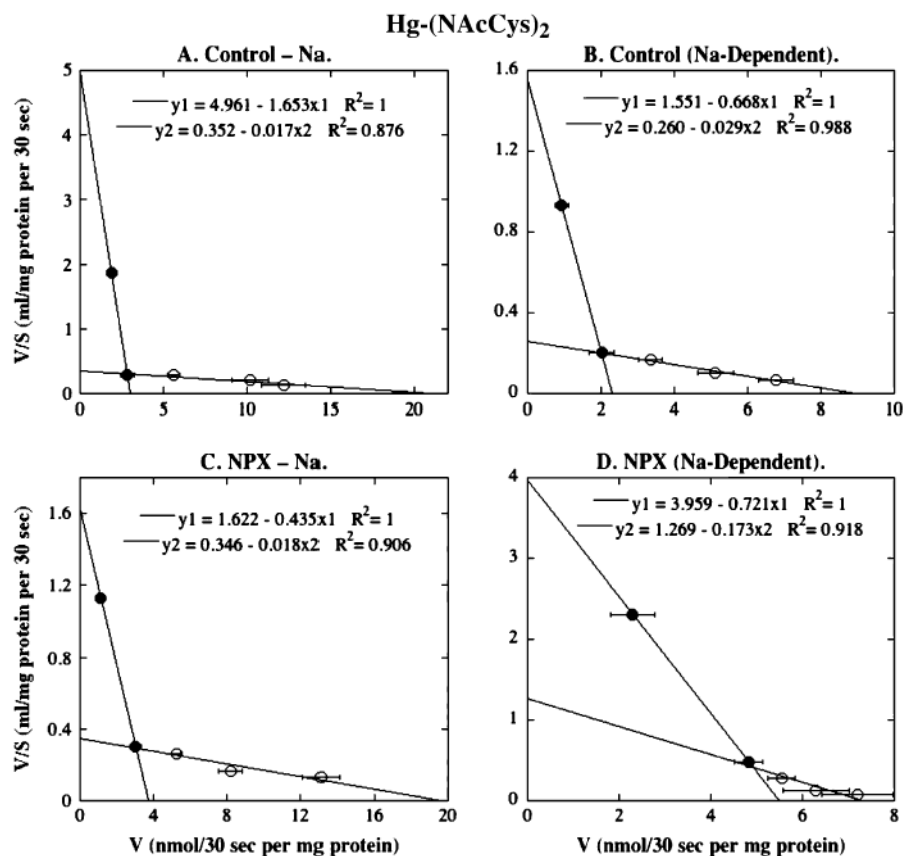
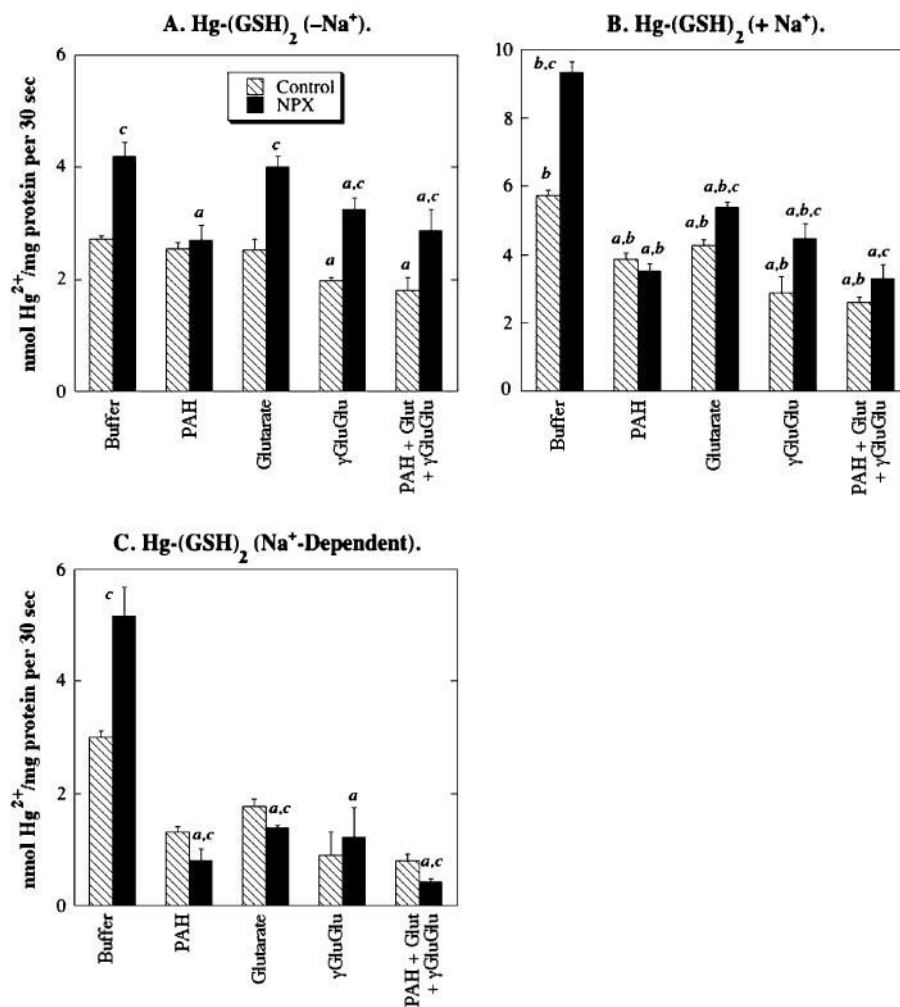
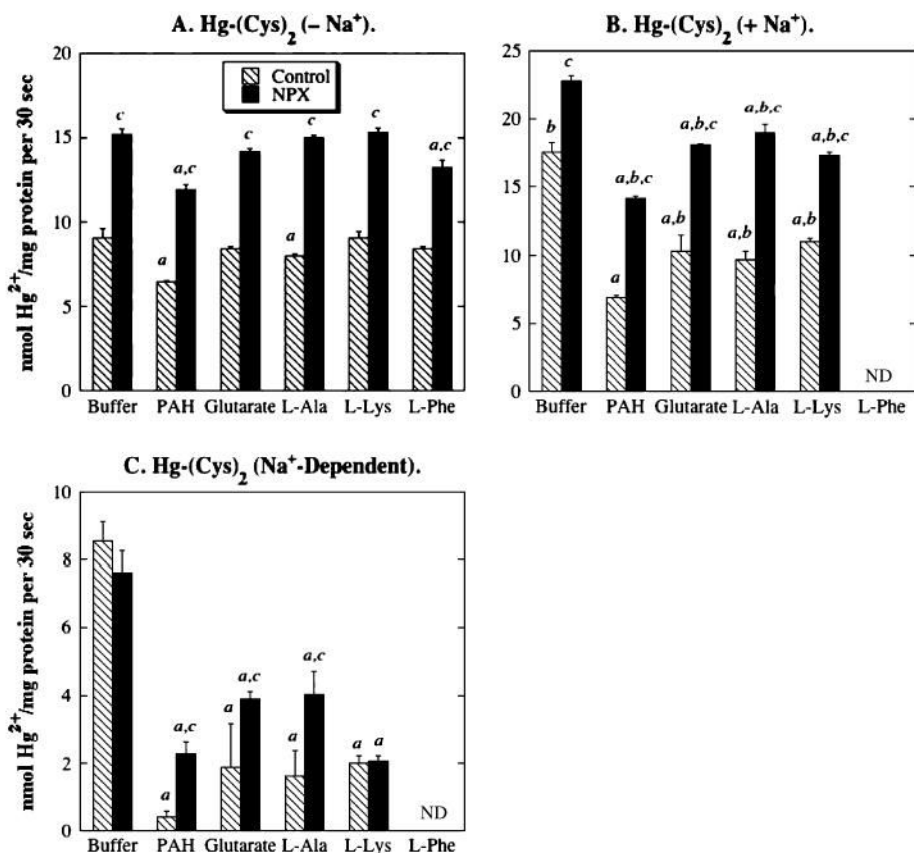


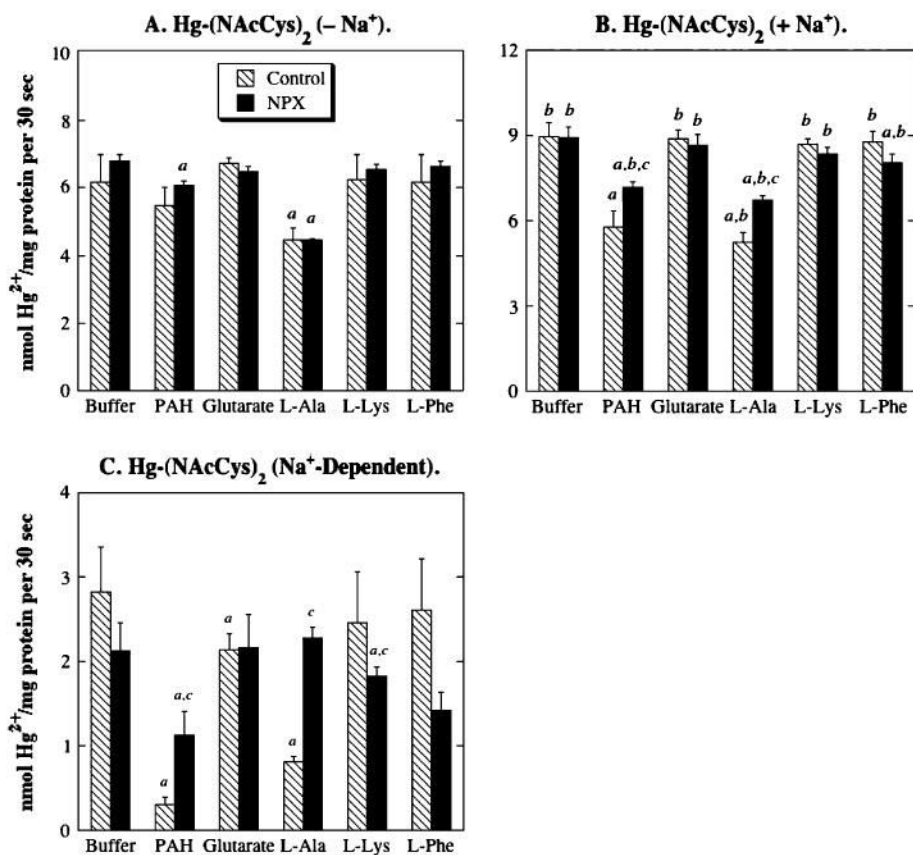
FIG. 7. Eadie-Hofstee plots for Hg-(NACys)₂ transport in BLM vesicles from control and NPX rat kidney(s). Initial rates of Hg-(NACys)₂ transport derived from Figure 3C for Na⁺-independent and Na⁺-dependent uptake were linearized by Eadie-Hofstee analysis and represent means \pm SE of measurements from separate membrane vesicle preparations from three control and three NPX rats. Where not visible, error bars were within the size of the data point. Filled and open symbols represent data points from different ranges that were selected to provide the best fit for linear regression.

**FIG. 8.**

Role of renal transporters in accumulation of Hg-(GSH)₂ in BLM vesicles from control and NPX rat kidney(s). Net accumulation of Hg-(GSH)₂ conjugate in BLM vesicles was determined by incubating vesicles with a pre-equilibrated solution of 20 μM HgCl₂ and 60 μM GSH, containing ²⁰³Hg²⁺, in the presence and absence of Na⁺ ions. When Na⁺ ions were present, potential competing substrates were added at a final concentration of 500 μM. Binding was subtracted from total intravesicular contents to give net uptake. Results, which indicate uptake in the absence of Na⁺ ions (-Na⁺), total uptake in the presence of Na⁺ ions (+Na⁺), and the Na⁺-dependent component of uptake, are expressed as nmol Hg²⁺/mg protein per 30 s and are means ± SE of measurements from separate membrane vesicle preparations from three control and three NPX rats. ^aStatistically significant difference (*p* < 0.05) from the corresponding sample incubated with buffer. ^bStatistically significant difference (*p* < 0.05) from the corresponding sample incubated in the absence of Na⁺ ions. ^cStatistically significant difference (*p* < 0.05) from the corresponding sample from BLM vesicles from control rat kidneys.

**FIG. 9.**

Role of renal transporters in accumulation of Hg-(Cys)₂ in BLM vesicles from control and NPX rat kidney(s). Net accumulation of Hg-(Cys)₂ conjugate in BLM vesicles was determined by incubating vesicles with a pre-equilibrated solution of 20 μM HgCl₂ and 60 μM L-cysteine, containing ²⁰³Hg²⁺, in the presence and absence of Na⁺ ions. Net accumulation values were determined as described in the legend to Figure 7. ^aStatistically significant difference ($p < 0.05$) from the corresponding sample incubated with buffer. ^bStatistically significant difference ($p < 0.05$) from the corresponding sample incubated in the absence of Na⁺ ions. ^cStatistically significant difference ($p < 0.05$) from the corresponding sample from BLM vesicles from control rat kidneys. ND, not determined.

**FIG. 10.**

Role of renal transporters in accumulation of Hg-(NACys)₂ in BLM vesicles from control and NPX rat kidney(s). Net accumulation of Hg-(NACys)₂ conjugate in BLM vesicles was determined by incubating vesicles with a pre-equilibrated solution of 20 μ M HgCl₂ and 60 μ M *N*-acetyl-L-cysteine, containing ²⁰³Hg²⁺, in the presence and absence of Na⁺ ions. Net accumulation values were determined as described in the legend to Figure 7. ^aStatistically significant difference ($p < 0.05$) from the corresponding sample incubated with buffer. ^bStatistically significant difference ($p < 0.05$) from the corresponding sample incubated in the absence of Na⁺ ions. ^cStatistically significant difference ($p < 0.05$) from the corresponding sample from BLM vesicles from control rat kidneys.

TABLE 1
Kinetic Parameters For Net Transport of Hg²⁺-Thiol Conjugates Across Isolated Basolateral Plasma Membrane (BLM) Vesicles from Kidneys of Control and NPX Rats

	Control		NPX	
	V _{max}	K _m	V _{max}	K _m
Hg-(GSH) ₂				
-Na ⁺				
System 1	3.50 ± 0.22	4.47 ± 0.25	3.85 ± 0.19	3.43 ± 0.24
System 2	9.27 ± 0.61	29.6 ± 1.7	11.5 ± 0.8	28.6 ± 1.5
Na ⁺ -dependent				
System 1	3.34 ± 0.20	8.82 ± 0.43	4.36 ± 0.18	1.98 ± 0.08
System 2	12.2 ± 0.5	85.9 ± 2.7	15.5 ± 0.7	41.6 ± 1.9
Hg-(Cys) ₂				
-Na ⁺				
System 1	7.42 ± 0.32	1.08 ± 0.07	11.1 ± 0.7	1.72 ± 0.06
System 2	21.6 ± 1.3	22.2 ± 1.0	24.8 ± 1.1	15.4 ± 0.6
Na ⁺ -dependent				
System 1	7.47 ± 0.95	3.26 ± 0.29	8.07 ± 0.66	0.88 ± 0.12
System 2	—	—	13.7 ± 1.1	9.11 ± 0.75
Hg-(NAcCys) ₂				
-Na ⁺				
System 1	3.00 ± 0.28	0.60 ± 0.05	3.73 ± 0.23	2.30 ± 0.11
System 2	21.0 ± 2.2	59.8 ± 4.8	19.5 ± 0.6	56.4 ± 1.8
Na ⁺ -dependent				
System 1	2.32 ± 0.13	1.50 ± 0.06	5.54 ± 0.76	1.40 ± 1.5
System 2	8.96 ± 0.35	34.4 ± 2.1	7.36 ± 0.62	5.79 ± 0.44

Note. Eadie-Hofstee plots of net Hg²⁺ accumulation data (-Na⁺ and Na⁺-dependent uptake) were derived from data presented in Figure 4 for Hg-(GSH)₂, Hg-(Cys)₂, and Hg-(NAcCys)₂ and are shown in Figures 5–7. In all cases but one, Eadie-Hofstee plots could discriminate between two carrier-mediated processes. Results are derived from experiments with membrane vesicles from three control or three NPX rat kidneys. V_{max} values are expressed as nmol/30 s per milligram of protein, and K_m values are expressed as μM Hg²⁺-thiol.